Zuse Institute Berlin

Takustrasse 7
D-14195 Berlin-Dahlem
Germany

POOJA GUPTA[a,c], ANNIKA GRAMATKE[b],
RALF EINSPANIER[b], CHRISTOF SCHÜTTE[a,c],
MAX VON KLEIST[a], JUTTA SHARBATI[b]

[a] *Department of Mathematics and Informatics, Freie Universität Berlin, Germany*

[b] *Department of Veterinary Biochemistry, Freie Universität Berlin, Germany*

[c] *Department of Mathematics for Life and Materials Sciences, Zuse Institute Berlin, Germany*

In silico cytotoxicity assessment on cultured rat intestinal cells deduced from cellular impedance measurements

ZIB Report 17-08 (Februar 2017)

Zuse Institute Berlin
Takustrasse 7
D-14195 Berlin-Dahlem

Telefon: 030-84185-0
Telefax: 030-84185-125

e-mail: bibliothek@zib.de
URL: http://www.zib.de

ZIB-Report (Print) ISSN 1438-0064
ZIB-Report (Internet) ISSN 2192-7782

In silico cytotoxicity assessment on cultured rat intestinal cells deduced from cellular impedance measurements

P. Gupta[a,c,*], A. Gramatke[b], R. Einspanier[b], C. Schütte[a,c], M.von Kleist[a,2], J. Sharbati[b,1,2]

[a]*Department of Mathematics and Informatics, Freie Universität Berlin, Arnimallee 6, 14195 Berlin, Germany*
[b]*Department of Veterinary Biochemistry, Freie Universität Berlin, Oertzenweg 19b, Building 12, 14163 Berlin*
[c]*Department of Mathematics for Life and Materials Sciences, Zuse Institute Berlin, Takustrasse 7, 14195 Berlin, Germany*

Abstract

Early and reliable identification of chemical toxicity is of utmost importance. At the same time, reduction of animal testing is paramount. Therefore, methods that improve the interpretability and usability of *in vitro* assays are essential. xCELLigence's real-time cell analyzer (RTCA) provides a novel, fast and cost effective *in vitro* method to probe compound toxicity. We developed a simple mathematical framework for the *qualitative* and *quantitative* assessment of toxicity for RTCA measurements. Compound toxicity, in terms of its 50% inhibitory concentration IC_{50} on cell growth, and parameters related to cell turnover were estimated on cultured IEC-6 cells exposed to 10 chemicals at varying concentrations. Our method estimated IC_{50} values of 113.05, 7.16, 28.69 and 725.15 μM for the apparently toxic compounds 2-acetylamino-fluorene, aflatoxin B1, benzo-[a]-pyrene and chloramphenicol in the tested cell line, in agreement with literature knowledge. IC_{50} values of all apparent *in vivo* non-toxic compounds were estimated to be non-toxic by our method. Corresponding estimates from RTCA's in-built model gave false positive (toxicity) predictions in 5/10 cases. Taken together, our proposed method reduces false positive predictions and reliably identifies chemical toxicity based on impedance measurements. The source code for the developed method including instructions is available at https://git.zib.de/bzfgupta/toxfit/tree/master.

Keywords: Real-time cell analyzer, Toxicity, Mathematical modeling, IC_{50}

1. Introduction

Identifying adverse effects of chemicals with respect to their distinguishing temporal and dose-dependent mode of action denotes a formidable challenge in toxicological research. Often, however, identifying toxic effects is rather difficult since indirect and long-term effects on both humans and the environment are not easy to assess, require an

*Corresponding author
Email addresses: gupta@math.fu-berlin.de (P. Gupta), annikagramatke@gmx.de (A. Gramatke), Ralf.Einspanier@fu-berlin.de (R. Einspanier), Christof.Schuette@fu-berlin.de (C. Schütte), vkleist@zedat.fu-berlin.de (M.von Kleist), Jutta.Sharbati@fu-berlin.de (J. Sharbati)
[1]Present address: Lise Meitner School of Science, Rudower Str. 184, 12351 Berlin, Germany
[2]equally contributed

immense investment of resources, and moreover, systematic testing itself may be unethical. Consequently, information about the hazards posed by a vast array of chemical substances is lacking (Schoeters, 2010).

A typical test routine for the prediction of toxicity relies on a sequence of stringent *in vitro* assays and *in vivo* experiments. Established mammalian cell-based *in vitro* assays for toxicity testing produce a high number of false positive results (Kirkland et al., 2007). Note, that any positive *in vitro* toxicity result leads to successive animal (*in vivo*) testing for validation. In order to avoid unnecessary animal testing, it is highly desirable to improve the predictive power of *in vitro* toxicity tests. Therefore, it is of utmost importance to integrate novel, resource-efficient approaches into testing strategies, which allow benchmarking the safety levels of substances and guide further experimentations.

The impedance-based xCELLigence real-time cell analyzer (RTCA) is an *in vitro* assay that provides a high-resolution temporal information about the physiological status of the cultivable attached cells such as cell number, morphology and adhesion. Upon treatment of cells with a toxic chemical, the impedance measurements (figure S1) change due to perturbation in the underlying cellular processes. Compounds with distinguishing RTCA profiles are therefore indicative of a characteristic mode of action (MoA) and the magnitude of drug effect on the cells (Abassi et al., 2009). The in-built RTCA software (Manual, 2009) uses a sigmoidal dose-response model which is fitted to impedance measurements at a particular time instance. However, a problem with this model is that it may produce small IC_{50}/EC_{50} values (indicating potent effects) even when the absolute magnitude of the change in impedance is small and possibly within the error of measurement, producing false positive predictions (figure 1). Thus, to delineate the precise relation of cellular response in context of different conditions (such as chemical concentration and time of administration) more reliability, application of mechanistic mathematical modeling is crucial.

Previous studies used clustering-based approaches for screening a library of chemical compounds on the basis of the RTCA profile (Abassi et al., 2009; Xi et al., 2014). Clustering-based methods provide a quick and reliable way of screening chemicals, but limitations are posed by the requirement of large training datasets and the test conditions (e.g. chemical concentrations used). Moreover, these methods may preclude a mechanistic insight into the chemicals' mode of action, as well as a quantitative characterization in terms of a dose-response profile. For a detailed insight into the chemicals' effect on the physiological dynamics of the cells, mechanistic modeling is required (Liang et al., 2014). Along these lines, Pan et al. (2013a,b) presented a two-exponent model for describing the cellular response towards toxic chemicals. More recently, Witzel et al. (2015) proposed a model for the growth curves of various colon cancer cells that allows predicting cell cycle time and IC_{50}. However, to the best of our knowledge, the aspect of mechanistic mathematical modeling has not yet been entirely explored with respect to predictive toxicology.

In this study, using the *in vitro* RTCA-based cell index data, we develop a methodology for quantifying the cytotoxicity of chemicals with known genotoxicity *in vivo*. As shown in figure 2, the RTCA-based cell index curves can be used to interpret the specific behavior of the cells (Kho et al., 2015). The initial period of the cell index curve illustrates the phase of cell adhesion and spreading (figure 2, left part). It is followed by a plateau phase prior to a gradual period of proliferation (Kho et al., 2015). Treatment with a chemical exposes the cells to an immediate

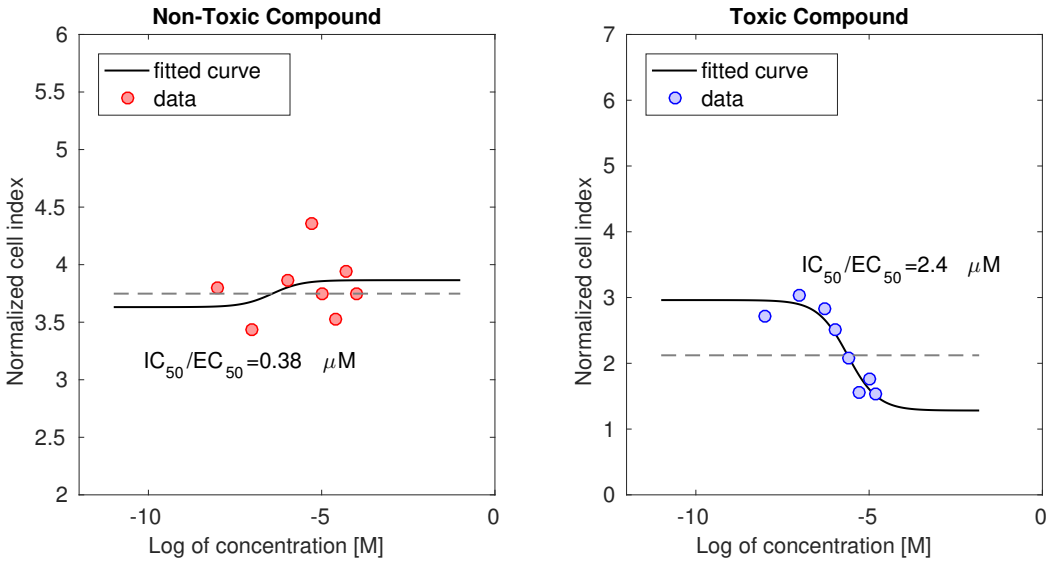

Figure 1: **Example fit.** Figure illustrates the fit of a simulated experimental data set to the in-built sigmoidal dose-response model. We simulated data without and with effect plus white noise for the non-toxic and toxic compound labelled in red and blue, respectively. A low estimate of IC_{50}/EC_{50} for the non-toxic compound (left panel) shows that the model produces a false positive result, although the absolute magnitude of change in cell index is small.

and transient phase of genotoxic effects (figure 2, middle part), which denote damage to the DNA arising from the specific MoA of the chemical (Scott et al., 1991). During this transient delay, cell cycle checkpoints are elicited in response to chemical treatment that allows cells to repair damage before progressing to the next phase of the cycle (Shackelford et al., 1999). Subsequently, the DNA damage accumulated during the genotoxic phase manifests in the form of cytotoxicity (figure 2, right part) representing an overall decline in cell survival and proliferation rate (Scott et al., 1991). Along these lines, we propose that the profiles from the cytotoxic phase can be used as a basis for the identification of test concentrations that are relevant for predicting chemical's genotoxicity *in vitro* and possibly *in vivo*.

In the presented work, we develop and validate an analytical framework to investigate the *in vitro* RTCA data on cultured IEC-6 cells for predicting cytotoxicity. We first propose a qualitative analysis based on the area under the curve to assess the relevance of the data for characterizing the toxicity of test chemicals. Thereafter, based on the insights obtained from this pre-analysis, a kinetic model is introduced for predicting the temporal- and dose-dependent effects of chemicals in terms of its 50% inhibitory concentration IC_{50} and parameters related to cell turnover, taking the actual cell impedance dynamics into account. The IC_{50} values obtained using our approach are compared to the values obtained using a sigmoidal dose-response model described in the RTCA software (Manual, 2009). By presenting a foundation work for modeling and analyzing the RTCA datasets for predicting cytotoxicity, we believe that the study will contribute to the goal of improving *in vitro* strategies for genotoxicity testing (Waters and Fostel, 2004).

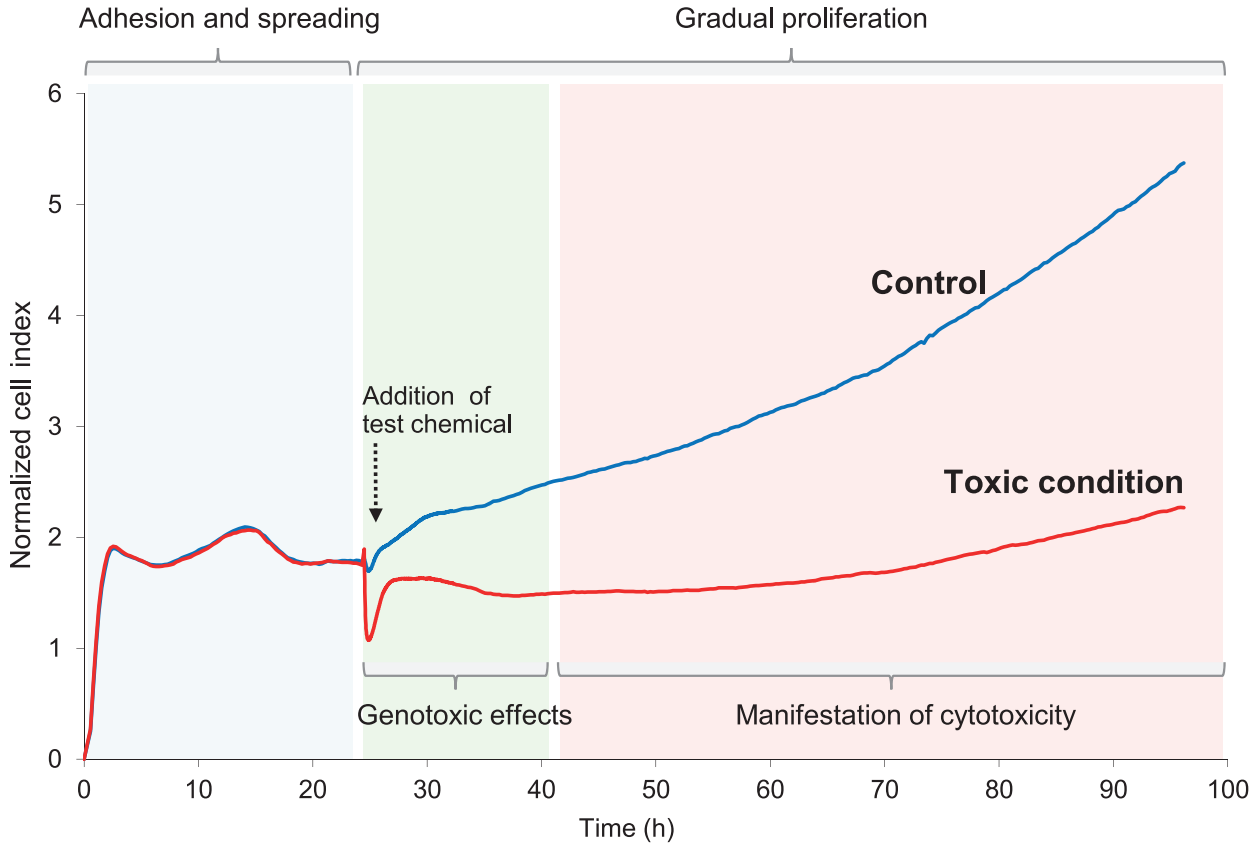

Figure 2: **Relationship between impedance measurement, genotoxic effects and their manifestation in terms of cytotoxicity.** Figure illustrates the change in cellular response upon exposure to a toxic chemical (red line) in comparison to normal condition (blue line). Upon addition of an apparently toxic chemical, the cells are exposed to the specific genotoxic effects attributed to the chemical's specific mode of action (MoA). Over a period of time, genotoxicity manifests in the form of cytotoxicity causing an overall decline in cell survival and proliferation rate. The cytotoxicity profile thus provides a basis for identifying test concentrations that are relevant for predicting MoA-based genotoxicity.

2. Methods

2.1. Chemicals

We evaluated 10 chemicals using a panel of test concentrations, summarized in table 1. In general, we used chemicals that are recommended for evaluating the sensitivity and specificity of novel mammalian cell genotoxicity assays (Kirkland et al., 2008). Importantly, these chemicals have been characterized for *in vivo* genotoxicity in rodents, and provide the possibility of correlating *in vitro* findings with existing *in vivo* data. Chemicals possessing tissue-specific genotoxicity *in vivo* included 2-acetylamino-fluorene, aflatoxin B1, benzo-[a]-pyrene, chloramphenicol and N-ethyl-N-nitrosourea. On the other hand, erythromycin, urea, D-mannitol, resorcinol and sulfisoxazole comprised chemicals that have not been found to exhibit genotoxicity. Non-genotoxic controls like urea, erythromycin and sulfisoxazole have been reported to produce false-positive results in *in vitro* genotoxicity

testing, despite clearly negative results *in vivo* (Kirkland et al., 2008). We chose to include these substances in order to account for the problem of false-positive testing.

The stock solution of the chemicals was prepared using their respective solvents (table 1). For preparing varying concentrations of the test chemicals, a dilution of the stock solution was carried out in a medium with 1% fetal calf serum (FCS; Biochrom AG) and dexamethasone. The solvent concentration, depending on the solubility of the chemical, was kept as low as possible to minimize the risk of solvent effects on impedance measurements.

Table 1: **Summary of chemicals**. List of test chemicals, their solvents and administered concentrations.

Chemical	Solvent	Test concentrations (μM)
2-Acetylamino-fluorene[a]	Ethanol	1, 10, 20, 30, 40, 50, 60, 70
Aflatoxin B1[a]	Dimethyl sulfoxide	0.01, 0.1, 0.5, 1, 2.5, 5, 10, 15
Benzo-[a]-pyrene[b]	Dimethyl sulfoxide	0.01, 0.1, 2.5, 10
Chloramphenicol[b]	Ethanol	1, 10, 20, 40, 60, 70, 80, 90
D-mannitol[b]	Water	0.01, 0.1, 1, 5, 10, 25, 50, 100
Erythromycin[b]	Ethanol	0.01, 0.1, 1, 5, 10, 25, 50, 100
N-ethyl-N-nitrosourea[b]	Water and ethanol (2:1)	0.01, 0.1, 1, 5, 10, 25, 50, 100
Resorcinol[b]	Water	0.01, 0.1, 1, 5, 10, 25, 50, 100
Sulfisoxazole[b]	Dimethyl sulfoxide	0.01, 0.1, 1, 5, 10, 25, 50, 100
Urea[b]	Water	0.01, 0.1, 1, 5, 10, 25, 50, 100

[a]purchased from Sigma Aldrich, Germany; [b]purchased from Carl Roth GmbH, Germany.

2.2. Cell culture

For the experiments, IEC-6 cell line (ATCC® CRL1592TM) originating from the small intestinal epithelium of *Rattus norwegicus* was used. Cell culture was performed in a medium containing 45% DMEM (4.5 g/l glucose with L-glutamine; Biochrom AG), 45% RPMI 1640 (Biochrom AG), 10% FCS, 0.1 units/ml bovine insulin (Sigma Aldrich) and 10 μg/ml gentamicin (Biochrom AG). Cells were incubated at 37 °C with 5% CO_2 and a relative humidity of 95%. For the xCELLigence assays, we supplemented the medium with 5 μM dexamethasone, which was found to be required to ensure proper cell growth on glass surfaces.

2.3. Real-time cell impedance measurement

For investigating the cytotoxicity of the test chemicals, a real-time cell analysis was performed using the xCELLigence System RTCA SP Station (ACEA Biosciences Inc.). A 96-well electronic microtiter plate (ACEA Biosciences Inc.) was used for seeding the cells in triplicates. Firstly, a calibration was performed with 50 μl medium and subsequently 50 μl cell suspension with a cell number of 1.5×10^5 cells per milliliter was added to obtain a cell number of approximately 7500 cells per well. After an incubation period of 24 h, the cells were treated with 50 μl solution containing the test chemicals listed in table 1. For the negative controls, cells were supplemented

with the medium after 24 h. In case of the solvent controls, cells were treated with the corresponding solvent not containing the test chemical.

Using xCELLigence's impedance-based measurements (expressed in terms of *cell index*), a surrogate estimate of viability and proliferation of the adhering cells (see figure 2) was obtained from the time of plating until the end of the experiment (96 h). Mean cell index values were calculated over the cell index values of the replicates for the control and chemically treated cultures and normalized as explained in the next paragraph.

2.4. Data normalization

To correct for the potentially different cell seeding, the values of cell index were normalized with respect to the cell index at the time of addition of the test chemical (24 h).

$$I(\tau, i, j) = \mathcal{I}(\tau, i, j)/\mathcal{I}(24, i, j) \tag{1}$$

where $I(\tau, i, j)$ is the normalized cell index value for the i^{th} chemical under the j^{th} experimental condition (concentration of test chemical) at the τ^{th} time-point. $\mathcal{I}(\tau, i, j)$ is the corresponding measured cell index value for that condition and $\mathcal{I}(24, i, j)$ is the measured cell index value at the time of chemical addition (24 h).

2.5. Qualitative Analysis

Preceding the modeling step, the cell-index data was analyzed by investigating the area under the cell-index curves (AUC). AUC estimates allowed a qualitative assessment of the toxicity of chemicals being investigated in the study. For example, in the presence of a cytotoxic chemical, a lower value of AUC indicated lower cell growth/higher cell death. AUC values were computed using the trapezoidal method (*trapz* function in MATLAB© version 8.4) for the cell-index curves obtained after exposure to the chemical. Estimates of AUC were acquired for negative control, solvent control and test chemicals. For a test chemical, AUC values were obtained for each of the test concentrations. From these values, the minimum value of AUC was selected, corresponding to the maximum observed toxic effect of the chemical, or in other words, the minimal growth of the cells.

2.6. Model

In the exponential growth phase of the cultured cells, the increase in the number of cells was modeled according to the following equation:

$$\hat{I}(t, i, j) = \hat{I}(t_0, i, j)e^{\lambda(i,j)t} \tag{2}$$

where $\hat{I}(t, i, j)$ and $\hat{I}(t_0, i, j)$ are the simulated cell indices for the i^{th} chemical at time $t \geq t_0$ and t_0, respectively, during the experimental condition j. $\lambda(i, j)$ is the net growth rate. t_0 denotes the time-point from which the data was used for parameter estimation (compare figure 2); we used $t_0 = 50$ h throughout the analysis.

In the model, $\lambda(i, j)$ is defined as a lumped parameter which is equal to the cell doubling rate minus the death rate of the cells. It incorporates the inhibitory effect of the chemical on cell growth in relation to different test concentrations, modeled via an Emax model (Ette and Williams, 2007):

$$\lambda(i, j) = \lambda_\phi(i)\frac{\mathrm{IC}_{50}(i)}{\mathrm{IC}_{50}(i) + D(i, j)} \tag{3}$$

where $\lambda_\phi(i)$ is the growth rate in the absence of the test chemical, $\mathrm{IC}_{50}(i)$ is the concentration of the chemical required to inhibit the cell growth by 50% and $D(i, j)$ denotes the administered concentration of the i^{th} chemical in the experiment.

2.7. Estimates of λ_ϕ and IC_{50}

Chemical-specific parameters, $\hat{I}(t_0, i, j)$, $\lambda_\phi(i)$, and IC_{50}(i), were estimated in a maximum likelihood sense by the optimization routine *lsqcurvefit* in MATLAB© version 8.4 using an ordinary least-squares criterion to minimize the residual error given as follows:

$$\theta^*(i) = \{I^*(t_0, i, j), \lambda^*_\phi(i), \mathrm{IC}^*_{50}(i)\} = argmin \sum_j \sum_t |\hat{I}(t, i, j) - I(t, i, j)|^2 \tag{4}$$

where $\hat{I}$ and I denote the estimated and experimental cell index values, respectively, and the superscript * indicates the optimal parameter estimate. Note that during parameter estimation, we implicitly assumed an additive normal distributed measurement error $\epsilon \sim N(0, \sigma^2)$ with $I = \hat{I} + \epsilon$.

2.8. Bootstrap sampling

We performed bootstrap resampling to assess the reliability of the parameter estimates. For 1000 iterations, data was resampled with replacement and parameter fitting was performed on each of the bootstrapped samples. Confidence intervals of the estimated parameters bounded by the 5^{th} and the 95^{th} percentiles were calculated from the resampling estimates.

2.9. RTCA's in-built dose-response model

To further validate the estimated IC_{50} values, we compared our results to the values obtained by fitting a sigmoidal dose-response model described in the RTCA software (Manual, 2009) provided by xCELLigence:

$$Y = y_0 + \frac{(y_1 - y_0)}{(1 + 10^{(LogIC_{50} - X)})} = y_0 + \frac{(y_1 - y_0) \cdot D}{(D + IC_{50})} \tag{5}$$

where, as recommended by the software (Manual, 2009), Y is either the normalized cell index at the last time point of the assay (equivalent to $I(t_{96}, i, j)$ above) or the AUC for the time-period between chemical administration and end of the assay. y_0 and y_1 are the baseline and plateau in the sigmoidal curve, respectively. X is the logarithm of the administered dose D. Depending on the specific action of the administered chemical (inducing or inhibiting), the above formula can be used to calculate the molar concentration of an inducer that produces 50% of the maximal possible cell index (EC_{50}) or an inhibitor that reduces the cell index by 50% (IC_{50}) (Neubig et al., 2003).

3. Results

3.1. Impedance measurements

For all 10 chemicals tested, the cellular-response profile was monitored continuously by the xCELLigence for 96 h from the time of plating of the IEC-6 cells until the end of the experiment. The mean normalized cell index of the control and chemically treated cultures are depicted in figure S1. A noticeable lowering of cell indices was observed in case of 2-acetylamino-fluorene, aflatoxin B1 and benzo-[a]-pyrene (figure S1). Additionally, depending on the dosage, these three chemicals had a wide ranging effect in comparison to the other tested chemicals.

3.2. AUC estimates

For all conditions, AUC values were calculated from the normalized cell index data (table 2). A comparison between the AUC values of the negative and solvent control showed that the cell index values did not change considerably indicating negligible solvent effects (table 2, middle column). The percentage change in the AUC values between the solvent control and the test chemical provided an initial inference about the influence of the test chemicals on cellular response (table 2, rightmost column). AUC based analysis indicated that 2-acetylamino-fluorene, aflatoxin B1, benzo-[a]-pyrene and chloramphenicol exhibit cytotoxic effects in comparison to the rest of the chemicals. N-ethyl-N-nitrosourea is a mutagenic compound used for inducing tumors, which preferentially manifests in the brain (Barth and Kaur, 2009). In the rat intestinal IEC-6 cell line used in our study it did not show any significant decline in AUC. On the other hand, the non-genotoxic compounds sulfisoxazole and resorcinol showed a slight decline in AUC. Therefore, for validating toxicity and overcoming a false positive/negative result, further evaluation of the chemicals was performed using the described *in silico* model.

Table 2: **AUC analysis.** Table showing percentage change in the area under the cell index curves for the control and the test chemicals.

Chemical	% change (SC[a] vs. NC[a])	% change (TC[a] vs. SC[a])
2-Acetylamino-fluorene	2.67	-61.25
Aflatoxin B1	4.44	-20.18
Benzo-[a]-pyrene	2.91	-19.14
Chloramphenicol	2.67	-13.45
D-mannitol	-3.33	-5.01
Erythromycin	-4.11	-2.96
N-ethyl-N-nitrosourea	5.35	-4.57
Resorcinol	8.34	-9.42
Sulfisoxazole	5.05	-10.54
Urea	1.54	-1.90

[a]NC, SC and TC denote negative control, solvent control and test chemical, respectively.

3.3. Parameter estimation

The response of the IEC-6 cell population under different concentrations of chemicals was fitted to the model described in the methods section to obtain the growth rate λ_ϕ and drug specific estimates of IC_{50}. Figure 3 illustrates the fit of the simulated and experimental data points for aflatoxin B1, benzo-[a]-pyrene, 2-acetylamino-fluorene and chloramphenicol, respectively. The results showed that aflatoxin B1, benzo-[a]-pyrene, 2-acetylamino-fluorene and chloramphenicol were cytotoxic, with respective IC_{50} values of 7 μM, 29 μM, 113 μM and 725 μM (table 3). For other chemicals, the estimates of IC_{50} approached very high values ($> 900\mu$M) such that their effect on the cell index kinetics can be considered insignificant at the tested concentration ranges (table 3 and figure S2). Similar to the AUC analysis, simulations also indicated that N-ethyl-N-nitrosourea was not cytotoxic within the administered concentration range. The mean growth rate (λ_ϕ) of the IEC-6 cells was estimated to be 0.0162 h^{-1}, i.e. a turn-over time of 2.6 days (table 4).

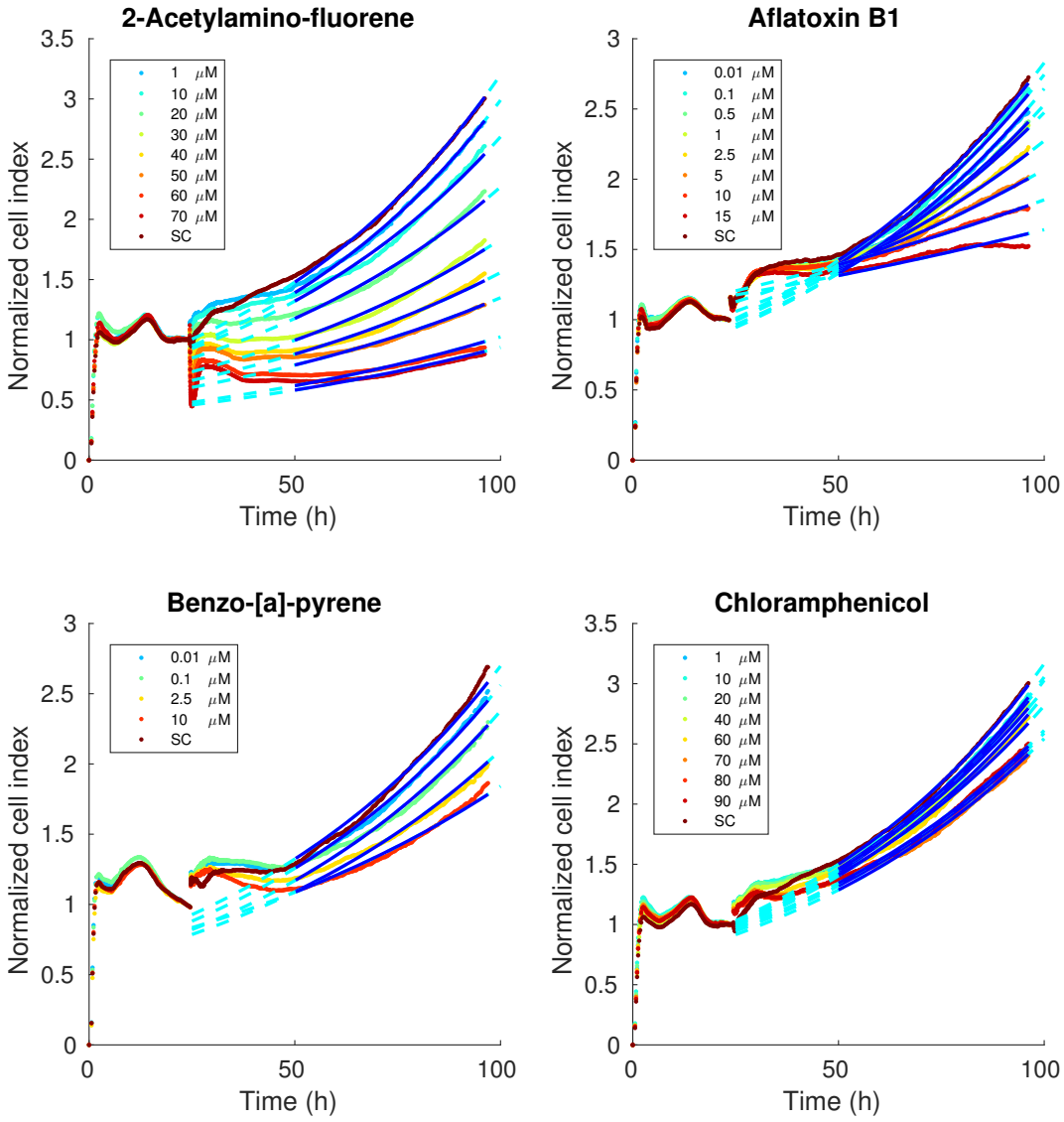

Figure 3: **Time-profiles of the simulated and the experimental data.** The figure depicts the fit of the simulated (in dark blue) and the experimental data (labeled colored markers in the sub-figures). Simulations were performed for the time-period relevant to the cytotoxic phase, which in our study was from 50 h until the end of the experiment. The cyan dashed line indicates the extrapolation of the simulated curves beyond the time-interval of simulations.

Table 3: **Summary of the estimated IC_{50} values (μM).** Table presents a summary of the IC_{50} estimate (in μM) using our model, including a comparison to the values from literature and RTCA's in-built model.

Chemical	IC_{50} using our model[a] [CI]	Literature[b]	In-built model[c]	IC_{50}/EC_{50}
			I	AUC
2-Acetylamino-fluorene	113.05 [109.24 - 117.64]	Cell-specific toxicity	37.75	50.28
Aflatoxin B1	7.16 [7.01 - 7.32]	Cell-specific toxicity	12.82	15.00
Benzo-[a]-pyrene	28.69 [26.48 - 31.28]	Cell-specific toxicity	0.17	1.52
Chloramphenicol	725.14 [679.39 - 778.68]	Antibiotic with adverse effects	486.90	667.06
D-mannitol	> 900[d]	Non-toxic at test concentrations	482.98	94.05
Erythromycin	> 900[d]	Non toxic at test concentrations	0.01	3.01
N-ethyl-N-nitrosourea	> 900[d]	Cell-specific toxicity at high-doses	9.21	8.12
Resorcinol	> 900[d]	Non-toxic at test concentrations	5.36×10^{7}	793.50
Sulfisoxazole	> 900[d]	Non-toxic at test concentrations	132.46	4.63×10^{-4}
Urea	> 900[d]	Non-toxic at test concentrations	19.71	0.18

[a]The second column shows estimates of IC_{50} with confidence intervals (CI) bounded by the 5^{th} and the 95^{th} percentiles based on our model. [b]The third column provides information about the toxicity of test chemicals as described in literature. A detailed interpretation is provided in the discussion section. [c]The fourth and fifth columns give estimates of IC_{50}/EC_{50} using RTCA's in-built sigmoidal dose-response model. The estimates are based on the normalized cell index values (I) and area under the dose-response curve (AUC). [d]Assuming that we observe insignificant (less than 10%) effect on growth at the highest test concentration (C_h), a lower-bound of IC_{50}/EC_{50} for the apparently non-toxic compounds was calculated from $0.1 > \frac{C_h}{C_h+IC_{50}} \Leftrightarrow IC_{50} > 10 \cdot C_h - C_h$.

Table 4: **Summary of the estimated growth rate.** The best estimates of growth rate of the IEC-6 cells with confidence intervals (CI) bounded by the 5^{th} and the 95^{th} percentiles are shown in the table.

Chemical	Growth rate (h^{-1}) [CI]
2-Acetylamino-fluorene	0.0154 [0.0154 - 0.0155]
Aflatoxin B1	0.0137 [0.0137 - 0.0138]
Benzo-[a]-pyrene	0.0142 [0.0141 - 0.0143]
Chloramphenicol	0.0149 [0.0149 - 0.0150]
D-mannitol	0.0154 [0.0153 - 0.0155]
Erythromycin	0.0154 [0.0153 - 0.0154]
N-ethyl-N-nitrosourea	0.0147 [0.0146 - 0.0147]
Resorcinol	0.0190 [0.0189 - 0.0191]
Sulfisoxazole	0.0190 [0.0189 - 0.0191]
Urea	0.0201 [0.0200 - 0.0202]
Average growth rate	0.0162 [0.0161 - 0.0163]

3.4. Comparison to RTCA's in-built model

Cell indices at the final time-point ($t = 96$) or AUC values were fitted to the model provided in the xCELLigence manual (eq. 5) in a maximum likelihood sense. The resulting IC_{50}/EC_{50} values are displayed in table 3. For apparently toxic compounds, the estimates of IC_{50} were in reasonable agreement with the predictions by our approach. However, for non-toxic compounds, the IC_{50}/EC_{50} values obtained by the sigmoidal dose-response model showed unrealistic values, indicating high potency (see table 3 and figure 4). The false positive predictions arise from the fact that the model is intrinsically prone to measurement noise. For example, a sigmoidal response is fit to the data, even when the magnitude of the absolute effect $|y_1 - y_o|$ is very small. Our model (eq. 2) overcomes these pitfalls.

4. Discussion

In this study, we presented an *in silico* modeling framework based on real-time cell impedance measurements in IEC-6 cells for predicting the cytotoxicity of chemicals. Intestinal cell lines are rarely studied in *in vitro* toxicology despite the intestinal epithelium being a site of massive exposure to xenobiotics after oral ingestion. Additionally, the intestine is considered to be the most important extrahepatic site of drug biotransformation (Thelen and Dressman, 2009), which can lead to the production of highly reactive metabolites in the gut wall. Regarding the tested chemicals, benzo-[a]-pyrene, aflatoxin B1 and 2-acetylamino-fluorene require intracellular bioactivation into mutagenic intermediates by cytochromes-P450 (CYPs) (Luch, 2005) to manifest their genotoxic effects. Since the expression of CYP enzymes is cell-specific, with cells contributing to first-pass clearance of foreign substances/toxins having the highest expression, the toxicity of these compounds is highly cell-specific and any *in vitro* assay based on cells not expressing relevant CYP enzymes will underestimate or fail to detect the toxicity of

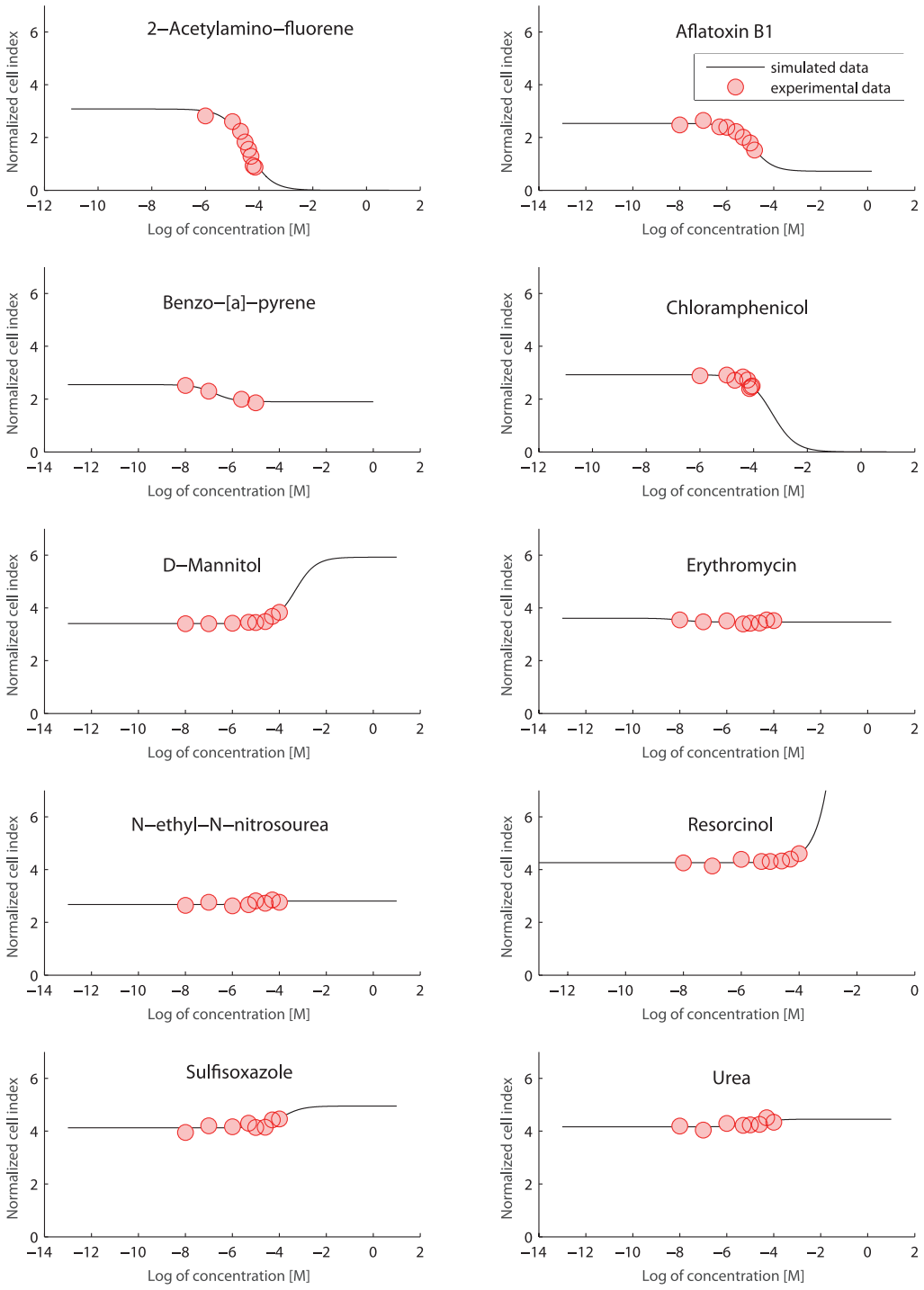

Figure 4: **RTCA's in-built dose-response model.** The figure illustrates the fit of the normalized cell index values at last time-point of the assay using RTCA's in-built dose-response model. The molar concentrations of the test chemicals are given in $\log_{10}$ scale.

these compounds. Therefore, an *in vitro* assessment of a dose- and temporal-based response in this cell line under relevant chemical exposure may provide critical data sets for the fundamental understanding of toxicity.

Using the RTCA assay, monitoring of cells started immediately after seeding. As a result, cells underwent an automatic quality-controlling even before the addition of test compounds; a measure that is usually not undertaken with standard endpoint assays of toxicity. On analyzing the data obtained from the RTCA assay, we observed temporal- and dose-dependent modifications in cell indices in relation to the cytotoxicity of the test chemical, as shown in figures 3 and S1. These variations in cell index at distinct time-instances suggest changes in the underlying molecular processes. Consequently, the cell index profile provides a useful basis for selecting relevant time-points for the application of successive in-depth experimental studies of toxicity. Furthermore, based on the RTCA profiles, we investigated the relationship between AUC and cytotoxicity. We observed that compounds with previously established genotoxicity, i.e. benzo-[a]-pyrene, chloramphenicol, 2-acetylamino-fluorene and aflatoxin B1, showed a decline in AUC relative to their corresponding solvent control, suggesting that a change in AUC allows compound classification into presumingly toxic versus non-toxic. However, the magnitude of change in AUC may not be used to compare different compounds quantitatively, or to rank them, since the magnitude of change can be different when the experiment is repeated (e.g. due to difference in seeding conditions, cell number etc.).

For predicting cytotoxicity, an *in silico* modeling approach was employed that investigated the changes in cellular kinetic profile capturing the pattern of cell growth in relation to temporal- and dose-dependent effects of the drug. As observed in the experimental data (figure S1), the cultured cells exhibited an initial genotoxicity specific lag-phase and a later cytotoxicity specific exponential-phase, with no noticeable growth saturation during the studied time-span. The cytotoxicity profiles present a fundamental basis for the identification of test concentrations that are relevant for predicting the genotoxic action of a chemical *in vitro* and *in vivo*. Therefore, we utilized the subsequent cytotoxicity-associated phase of growth for parameter inference and modeling; similar to (Witzel et al., 2015) emphasizing the use of an appropriate time-interval for accurately predicting cytotoxicity.

The estimates of intestinal epithelium turn-over time/growth rate were close to the biologically observed value of 2–6 days (Delgado et al., 2016) showing that the mathematical model correctly captured the cellular growth kinetics. In concordance with the AUC analysis, the estimates of IC_{50} from our model also indicated that 2-acetylamino-fluorene, aflatoxin B1, benzo-[a]-pyrene and chloramphenicol were cytotoxic to the considered cell line. Note that the IC_{50} value for a compound may vary for different cell lines, experimental conditions, analyzed endpoints and species. For 2-acetylamino-fluorene, aflatoxin B1, benzo-[a]-pyrene particular variations between different cell lines are expected, since these compounds undergo CYP-mediated intracellular transformation to produce the ultimate toxic moiety. Thus, depending on the availability and absolute intracellular expression of relevant CYP enzymes, distinct levels of cytotoxicity are expected.

Nonetheless, comparing against IC_{50} values from independent sources can be useful, given that the utilized cell lines permit such comparison. Genotoxicity of benzo-[a]-pyrene primarily depends on its endogenous biotransformation (e.g. into (+)-anti-BP-7,8-diol-9,10-epoxide). Biotransformation is controlled by the cell-type

specific expression of CYP1 (CYP1A1, CYP1A2 and CYP1B1) and other phase I/II enzymes (Luch, 2005; Nebert and Dalton, 2006). Therefore, its *in vitro* toxicity is likely to be different between CYP expressing cells (e.g. liver and intestinal cells) and cells that do not express relevant CYP enzymes. Unfortunately, to our knowledge no relevant data on the cytotoxicity of benzo-[a]-pyrene in rat intestinal cells is available. In liver cell lines, IC_{50} values of 0.04–38.04 μM have been reported (Payen et al., 2001; Rodrigues et al., 2013), where the former values were derived from F258 cells (rat liver epithelial cell line) and the latter from undifferentiated-HepaRG cells (human hepatoma cell line). In comparison, we estimated a value of 28.69 μM in our intestinal cell line. As expected, the use of cells that do not express significant amounts of CYP enzymes can result in an *underestimated* or *false negative* toxicity predictions (for example, Carfi' et al. (2007) used rat spleen cells and predicted a value of $> 200\mu$M). Likewise, aflatoxin B1 requires CYP-mediated activation to form cytotoxic and DNA-reactive intermediate aflatoxin-8,9-epoxide, mainly by CYP3A4 but also by CYP1A (Dohnal et al., 2014; Massey et al., 1995). Its metabolism and toxicity in intestinal cells is not fully investigated, but correlated with the CYP3A4 expression (Kolars et al., 1994). The most closely related cells in terms of relevant CYP expression, where literature data is available, are liver cells. The IC_{50} measured in primary liver cells was 0.3 μM (Hanigan and Laishes, 1984), which is, as expected (see above) slightly smaller than the value of 7.16 μM predicted in our study, given that the order of adduct formation within tissues was proposed to be liver>kidney>colon>lung=spleen (Cupid et al., 2004). The corresponding IC_{50} measured in the rat liver fibroblast cell line BRL 3A was 38 μM, which is slightly higher than our prediction and may be related to the relatively low expression of CYP enzymes in this cell line (Boess et al., 2003). 2-Acetylamino-fluorene undergoes transformation by the enzymes CYP1A1 and CYP1A2, and subsequently by acyl-transferase and sulfo-transferase into genotoxic electrophilic compounds, which react with DNA to form mutagenic adducts (Heflich and Neft, 1994). As in case of benzo-[a]-pyrene and aflatoxin B1, the distribution of DNA adducts in various tissues is a direct function of the metabolic capacity of the target cells. The highest adduct levels are often found in the liver, which contains high concentrations of enzymes important to the activation of 2-acetylamino-fluorene. Since the intestine is a site of first-pass metabolism, IC_{50} estimates in the studied IEC-6 cells (113.05 μM) are within a similar range to those observed in cell lines derived from rat liver (77 μM in cultured rat liver epithelial F258 cell (Sparfel et al., 2002) and 130 μM in RL1, an epithelial-like cell line derived from rat liver (Scott et al., 1991)). Unlike the previously mentioned compounds, chloramphenicol (a broad-spectrum antibiotic) does not need to undergo intracellular activation in order to exert its (weak) toxicity. The predicted value of 725.14 μM using our method and cell line is in good agreement with the literature 490–710 μM (Halle, 2003).

Our IC_{50} estimate for N-ethyl-N-nitrosourea indicated no cytotoxicity. N-ethyl-N-nitrosourea is a mutagenic compound, which is used as a tool for inducing tumors (Kirkland et al., 2008). Unlike the previously discussed chemicals, N-ethyl-N-nitrosourea decomposes heterolytically (without enzymatic involvement) with an intracellular half-life of < 8 min (Goth and Rajewsky, 1972). The ultimate reactant, an electrophilic ethyl cation inducing DNA damage, is thus produced indiscriminately in all tissues. However, toxicity has been observed to be tissue-specific *in vivo* in rats; preferentially affecting the brain cells (Barth and Kaur, 2009). The reason for a selective toxicity is

believed to be due to cell-specific differences in the DNA repair mechanism; i.e. DNA repair may insufficiently counteract DNA damage in brain cells (Müller and Rajewsky, 1983) whereas most cells have a high capacity for repairing N-ethyl-N-nitrosourea induced DNA damage (Loquet and Wiebel, 1982). As a result, most *in vitro* studies on rat utilized cells derived from the central nervous system for testing N-ethyl-N-nitrosourea's toxicity. These studies indicate IC_{50} values greater than 450 μM ((Kidney and Faustman, 1995)), which given the arguments above are expected to be much higher in other cell lines including the tested IEC-6 cell line (IC_{50} values were reported to be $>$ 1 mM by Driscoll et al. (1995); Sehlmeyer and Wobus (1994); Elsner et al. (2000)). Given the low test concentrations in the range of 0.01–100 μM in our study, we therefore did not observe cytotoxicity in IEC-6 cells. Interestingly, the RTCA in-built model, in contrast, predicted a very low IC_{50} which is an artifact and a false positive result under the investigated test condition.

The IC_{50} values of all apparent *in vivo* non-toxic compounds were estimated to be non-toxic ($>$ 900 μM) by our method. It is also evident from the non-saturating dose-reponse curves for all non-toxic compounds (figure 4) that these compounds did not manifest any cytotoxic effect on the cell. In contrast, RTCA's in-built sigmoidal dose-response model for estimating IC_{50}/EC_{50} gave unrealistically low values (false-positively indicating toxicity) for compounds which are considered to be non-toxic. The reason is that for a compound with little or no apparent effect (difference between the baseline and plateau level), RTCA's in-built dose-response model will always enforce a sigmoidal response curve, deducing some values of IC_{50}/EC_{50}, even if the RTCA endpoints were derived under non-saturating conditions. This is in fact a major downside of RTCA's in-built model, which makes it prone to predict low values of IC_{50} (false positives) for non-toxic compounds. Our model, on the other hand, simulates the actual time trajectories of cellular growth and captures the kinetics of chemical action, thereby giving robust estimates and reducing false positive test results. If the compound has no effect on the RTCA profiles and the corresponding dose-response curve does not exhibit saturation for the tested concentration range, very high values (indicating no toxicity under test conditions) of IC_{50} values are thus estimated by our model. Since a high IC_{50} value (far from the biologically relevant concentration range) indicates no observed cytotoxicity, our model reduces artifacts and false positive predictions generated by RTCA's in-built sigmoidal dose-response model for non-toxic compounds.

Our aim was to reliably identify chemical toxicity, considering that *in vitro* toxicity tests are a major contributor to false-positive results in genotoxicity testing. Our method eliminates many false positive results, and enables the design of subsequent genotoxicity tests that considers cytotoxicity in a time- and concentration-resolved manner. However, great caution needs to be taken when choosing appropriate cell lines as observed in this study, since many toxic moieties (e.g. benzo-[a]-pyrene, aflatoxin B1 and 2-acetylamino-fluorene) may be generated by enzymes which are differently expressed across cell types. Moreover, cellular detoxification and repair mechanisms can be cell-specific as well, which is likely the case for N-ethyl-N-nitrosourea. As a consequence, systemic, or tissue dependent *in vivo* toxicity can deviate substantially from observed *in vitro* toxicity, depending on the choice of the cell line studied.

5. Conclusion

To summarize, using our mathematical framework for the qualitative and quantitative assessment of the RTCA measurements, useful insights were obtained regarding chemicals' toxicity and IEC-6 cells' growth kinetics. Instead of utilizing an empirical mathematical model, a simple mechanistic model of cell growth inhibition was developed that quantified toxicity in terms of the biologically interpretable parameter IC_{50}, a measure utilized by most experimenters. The quantitative modeling approach in conjunction with the qualitative AUC analysis yielded valuable information about the time- and concentration-specific effects of the tested chemicals. The results showed that the proposed mathematical model predicted the IC_{50} and the growth rates of the cultured cells in agreement with biological knowledge. This demonstrates that *in silico* models are crucial for testing toxicity of chemicals, especially for overcoming spurious false positive results. Finally, bearing in mind the limitations of the current study, in future we aim to direct our approach towards developing more advanced models and generating complementary experimental datasets allowing to assess in depth the mode of action of drugs. The source code for the developed method including instructions is available at https://git.zib.de/bzfgupta/toxfit/tree/master.

Acknowledgments

We would like to acknowledge financial support from the Freie Universität Berlin within the Excellence Initiative of the German Research Foundation, the Forschungskommission of Freie Universität Berlin and the BMBF-funded research group Meth4SysPharm, grant number 031A307. In addition, this work was partly funded by the GRACE project ('GMO Risk Assessment and Communication of Evidence'), financially supported by the 7th Framework Program of the European Community for Research, Technological Development and Demonstration Activities (FP7), Grant Agreement no. 311957. We would also like to express our gratitude to Dr. S. Sharbati for the helpful suggestions.

References

Abassi, Y.A., Xi, B., Zhang, W., Ye, P., Kirstein, S.L., Gaylord, M.R., Feinstein, S.C., Wang, X., Xu, X., 2009. Kinetic cell-based morphological screening: Prediction of mechanism of compound action and off-target effects. Chemistry and Biology 16, 712–723. doi:10.1016/j.chembiol.2009.05.011.

Barth, R.F., Kaur, B., 2009. Rat brain tumor models in experimental neuro-oncology: the C6, 9L, T9, RG2, F98, BT4C, RT-2 and CNS-1 gliomas. Journal of neuro-oncology 94, 299–312. doi:10.1007/s11060-009-9875-7.

Boess, F., Kamber, M., Romer, S., Gasser, R., Muller, D., Albertini, S., Suter, L., 2003. Gene expression in two hepatic cell lines, cultured primary hepatocytes, and liver slices compared to the in vivo liver gene expression in rats: possible implications for toxicogenomics use of in vitro systems. Toxicological sciences : an official journal of the Society of Toxicology 73, 386–402. doi:10.1093/toxsci/kfg064.

Carfi', M., Gennari, A., Malerba, I., Corsini, E., Pallardy, M., Pieters, R., Loveren, H.V., Vohr, H., Hartung, T., Gribaldo, L., 2007. In vitro tests to evaluate immunotoxicity: A preliminary study. Toxicology 229, 11 – 22. doi:10.1016/j.tox.2006.09.003.

Cupid, B.C., Lightfoot, T.J., Russell, D., Gant, S.J., Turner, P.C., Dingley, K.H., Curtis, K.D., Leveson, S.H., Turteltaub, K.W., Garner, R.C., 2004. The formation of AFB_1-macromolecular adducts in rats and humans at dietary levels of exposure. Food and chemical toxicology : an international journal published for the British Industrial Biological Research Association 42, 559–569. doi:10.1016/j.fct.2003.10.015.

Delgado, M.E., Grabinger, T., Brunner, T., 2016. Cell death at the intestinal epithelial front line. The FEBS Journal 283, 2701–2719. doi:10.1111/febs.13575.

Dohnal, V., Wu, Q., Kua, K., 2014. Metabolism of aflatoxins: key enzymes and interindividual as well as interspecies differences. Archives of toxicology 88, 1635–1644. doi:10.1007/s00204-014-1312-9.

Driscoll, K.E., Deyo, L.C., Howard, B.W., Poynter, J., Carter, J.M., 1995. Characterizing mutagenesis in the hprt gene of rat alveolar epithelial cells. Experimental Lung Research 21, 941956. doi:10.3109/01902149509031772.

Elsner, M., Guldbakke, B., Tiedge, M., Munday, R., Lenzen, S., 2000. Relative importance of transport and alkylation for pancreatic beta-cell toxicity of streptozotocin. Diabetologia 43, 15281533. doi:10.1007/s001250051564.

Ette, E.I., Williams, P.J. (Eds.), 2007. Pharmacometrics: The science of quantitative Pharmacology. John Wiley & Sons.

Goth, R., Rajewsky, M.F., 1972. Ethylation of nucleic acids by ethylnitrosourea-1-^{14}C in the fetal and adult rat. Cancer research 32, 1501–1505.

Halle, W., 2003. The registry of cytotoxicity: toxicity testing in cell cultures to predict acute toxicity (LD50) and to reduce testing in animals. Alternatives to laboratory animals 31, 89–198.

Hanigan, H.M., Laishes, B.A., 1984. Toxicity of aflatoxin B_1 in rat and mouse hepatocytes in vivo and in vitro. Toxicology 30, 185–193. doi:10.1016/0300-483X(84)90090-8.

Heflich, R.H., Neft, R.E., 1994. Genetic toxicity of 2-acetylaminofluorene, 2-aminofluorene and some of their metabolites and model metabolites. Mutation research 318, 73–114. doi:10.1016/0165-1110(94)90025-6.

Kho, D., MacDonald, C., Johnson, R., Unsworth, C.P., O'Carroll, S.J., Mez, E.d., Angel, C.E., Graham, E.S., 2015. Application of xCELLigence RTCA biosensor technology for revealing the profile and window of drug responsiveness in real time. Biosensors 5, 199–222. doi:10.3390/bios5020199.

Kidney, J., Faustman, E., 1995. Modulation of nitrosourea toxicity in rodent embryonic cells by O^6-Benzylguanine, a depletor of O^6-methylguanine-DNA methyltransferase. Toxicology and Applied Pharmacology 133, 111. doi:10.1006/taap.1995.1120.

Kirkland, D., Kasper, P., Müller, L., Corvi, R., Speit, G., 2008. Recommended lists of genotoxic and non-genotoxic chemicals for assessment of the performance of new or improved genotoxicity tests: A follow-up to an ECVAM workshop. Mutation Research/Genetic Toxicology and Environmental Mutagenesis 653, 99–108. doi:10.1016/j.mrgentox.2008.03.008.

Kirkland, D., Pfuhler, S., Tweats, D., Aardema, M., Corvi, R., Darroudi, F., Elhajouji, A., Glatt, H., Hastwell, P., Hayashi, M., Kasper, P., Kirchner, S., Lynch, A., Marzin, D., Maurici, D., Meunier, J.R., Müller, L., Nohynek, G., Parry, J., Parry, E., Thybaud, V., Tice, R., van Benthem, J., Vanparys, P., White, P., 2007. How to reduce false positive results when undertaking in vitro genotoxicity testing and thus avoid unnecessary follow-up animal tests: Report of an ECVAM workshop. Mutation Research/Genetic Toxicology and Environmental Mutagenesis 628, 31–55. doi:10.1016/j.mrgentox.2006.11.008.

Kolars, J.C., Benedict, P., Schmiedlin-Ren, P., Watkins, P.B., 1994. Aflatoxin B1-adduct formation in rat and human small bowel enterocytes. Gastroenterology 106, 433–439. doi:10.1016/0016-5085(94)90602-5.

Liang, Q., Gao, X., Chen, Y., Hong, K., Wang, H.S., 2014. Cellular mechanism of the nonmonotonic dose response of bisphenol A in rat cardiac myocytes. Environmental Health Perspectives 122, 601–608. doi:10.1289/ehp.1307491.

Loquet, C., Wiebel, F., 1982. Geno- and cytotoxicity of nitrosamines, aflatoxin b1, and benzo[a]-pyrene in continuous cultures of rat hepatoma cells. Carcinogenesis 3, 12131218. doi:10.1093/carcin/3.10.1213.

Luch, A., 2005. Nature and nurture - lessons from chemical carcinogenesis. Nat Rev Cancer 5, 113–125. doi:10.1038/nrc1546.

Manual, 2009. RTCA Software Manual, Software Version 1.2. URL: http://sydney.edu.au/medicine/bosch/facilities/molecular-biology/tissue-culture/RTCA%201.2%20Software%20Manual.pdf.

Massey, T.E., Stewart, R.K., Daniels, J.M., Liu, L., 1995. Biochemical and molecular aspects of mammalian susceptibility to aflatoxin B_1 carcinogenicity. Proceedings of the Society for Experimental Biology and Medicine. Society for Experimental Biology and Medicine (New

York, N.Y.) 208, 213–227. doi:10.3181/00379727-208-43852A.

Müller, R., Rajewsky, M.F., 1983. Elimination of O^6-ethylguanine from the DNA of brain, liver, and other rat tissues exposed to ethylnitrosourea at different stages of prenatal development. Cancer research 43, 2897–2904.

Nebert, D.W., Dalton, T.P., 2006. The role of cytochrome p450 enzymes in endogenous signalling pathways and environmental carcinogenesis. Nature Reviews Cancer 6, 947960. doi:10.1038/nrc2015.

Neubig, R.R., Spedding, M., Kenakin, T., Christopoulos, A., 2003. International union of pharmacology committee on receptor nomenclature and drug classification. XXXVIII. update on terms and symbols in quantitative pharmacology. Pharmacological Reviews 55, 597–606. doi:10.1124/pr.55.4.4.

Pan, T., Huang, B., Zhang, W., Gabos, S., Huang, D.Y., Devendran, V., 2013a. Cytotoxicity assessment based on the AUC_{50} using multi-concentration time-dependent cellular response curves. Analytica Chimica Acta 764, 44–52. doi:10.1016/j.aca.2012.12.047.

Pan, T., Khare, S., Ackah, F., Huang, B., Zhang, W., Gabos, S., Jin, C., Stampfl, M., 2013b. In vitro cytotoxicity assessment based on KC_{50} with real-time cell analyzer (RTCA) assay. Computational Biology and Chemistry 47, 113–120. doi:10.1016/j.compbiolchem.2013.08.008.

Payen, L., Courtois, A., Langout, S., Guillouzo, A., Fardel, O., 2001. Unaltered expression of multidrug resistance transporters in polycyclic aromatic hydrocarbon-resistant rat liver cells. Toxicology 156, 109 – 117. doi:10.1016/S0300-483X(00)00348-6.

Rodrigues, R.M., Bouhifd, M., Bories, G., Sacco, M.G., Gribaldo, L., Fabbri, M., Coecke, S., Whelan, M.P., 2013. Assessment of an automated in vitro basal cytotoxicity test system based on metabolically-competent cells. Toxicology in Vitro 27, 760 – 767. doi:10.1016/j.tiv.2012.12.004.

Schoeters, G., 2010. The reach perspective: Toward a new concept of toxicity testing. Journal of Toxicology and Environmental Health, Part B 13, 232–241. doi:10.1080/10937404.2010.483938.

Scott, D., Galloway, S.M., Marshall, R.R., Ishidate, M., Brusick, D., Ashby, J., Myhr, B.C., 1991. Genotoxicity under extreme culture conditions. Mutation Research/Reviews in Genetic Toxicology 257, 147 – 205. doi:10.1016/0165-1110(91)90024-P.

Sehlmeyer, U., Wobus, A.M., 1994. Lower mutation frequencies are induced by ENU in undifferentiated embryonic cells than in differentiated cells of the mouse in vitro. Mutation Research Letters 324, 69 – 76. doi:10.1016/0165-7992(94)90070-1.

Shackelford, R.E., Kaufmann, W.K., Paules, R.S., 1999. Cell cycle control, checkpoint mechanisms, and genotoxic stress. Environmental Health Perspectives 107, 5–24. doi:10.2307/3434468.

Sparfel, L., Loewert, M., Huc, L., Payen, L., Guillouzo, A., Lagadic-Gossmann, D., Fardel, O., 2002. Acute cytotoxicity of the chemical carcinogen 2-acetylaminofluorene in cultured rat liver epithelial cells. Toxicology Letters 129, 245–254. doi:10.1016/S0378-4274(02)00015-2.

Thelen, K., Dressman, J.B., 2009. Cytochrome p450-mediated metabolism in the human gut wall. Journal of Pharmacy and Pharmacology 61, 541–558. doi:10.1211/jpp.61.05.0002.

Waters, M.D., Fostel, J.M., 2004. Toxicogenomics and systems toxicology: aims and prospects. Nature Reviews Genetics 5, 936–948. doi:10.1038/nrg1493.

Witzel, F., Fritsche-Guenther, R., Lehmann, N., Sieber, A., Blüthgen, N., 2015. Analysis of impedance-based cellular growth assays. Bioinformatics 31, 2705–2712. doi:10.1093/bioinformatics/btv216.

Xi, Z., Khare, S., Cheung, A., Huang, B., Pan, T., Zhang, W., Ibrahim, F., Jin, C., Gabos, S., 2014. Mode of action classification of chemicals using multi-concentration time-dependent cellular response profiles. Computational Biology and Chemistry 49, 23–35. doi:10.1016/j.compbiolchem.2013.12.004.

Supplementary files

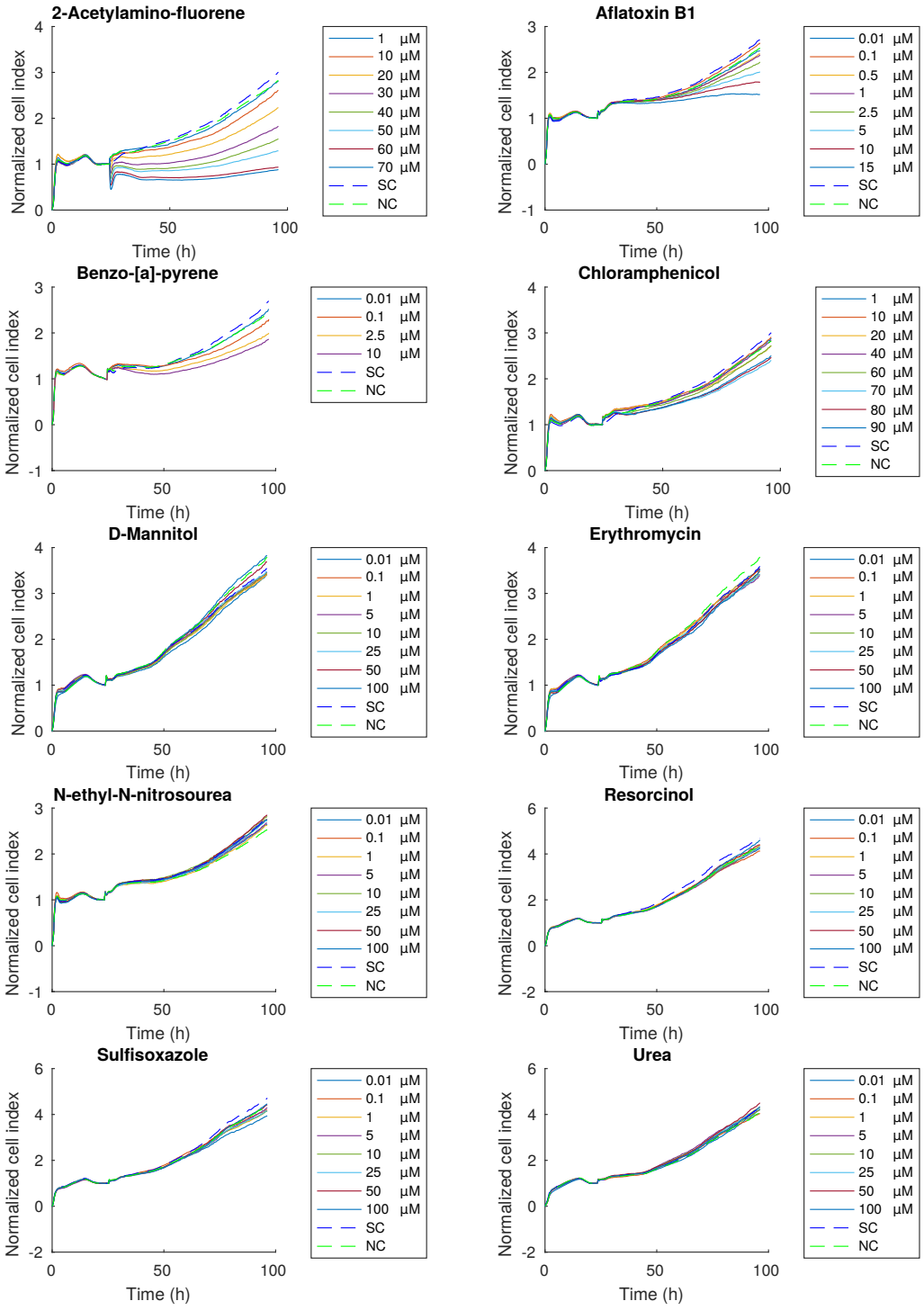

Figure S1: **Normalized cell index curves.** The plots depict the normalized cell index values upon treatment with different concentrations of test chemicals (i.e. 2-acetylamino-fluorene, aflatoxin B1, benzo-[a]-pyrene, chloramphenicol, D-mannitol, erythromycin, N-ethyl-N-nitrosourea, resorcinol, sulfisoxazole and urea) during 96 h. SC and NC denote solvent and negative controls, respectively.

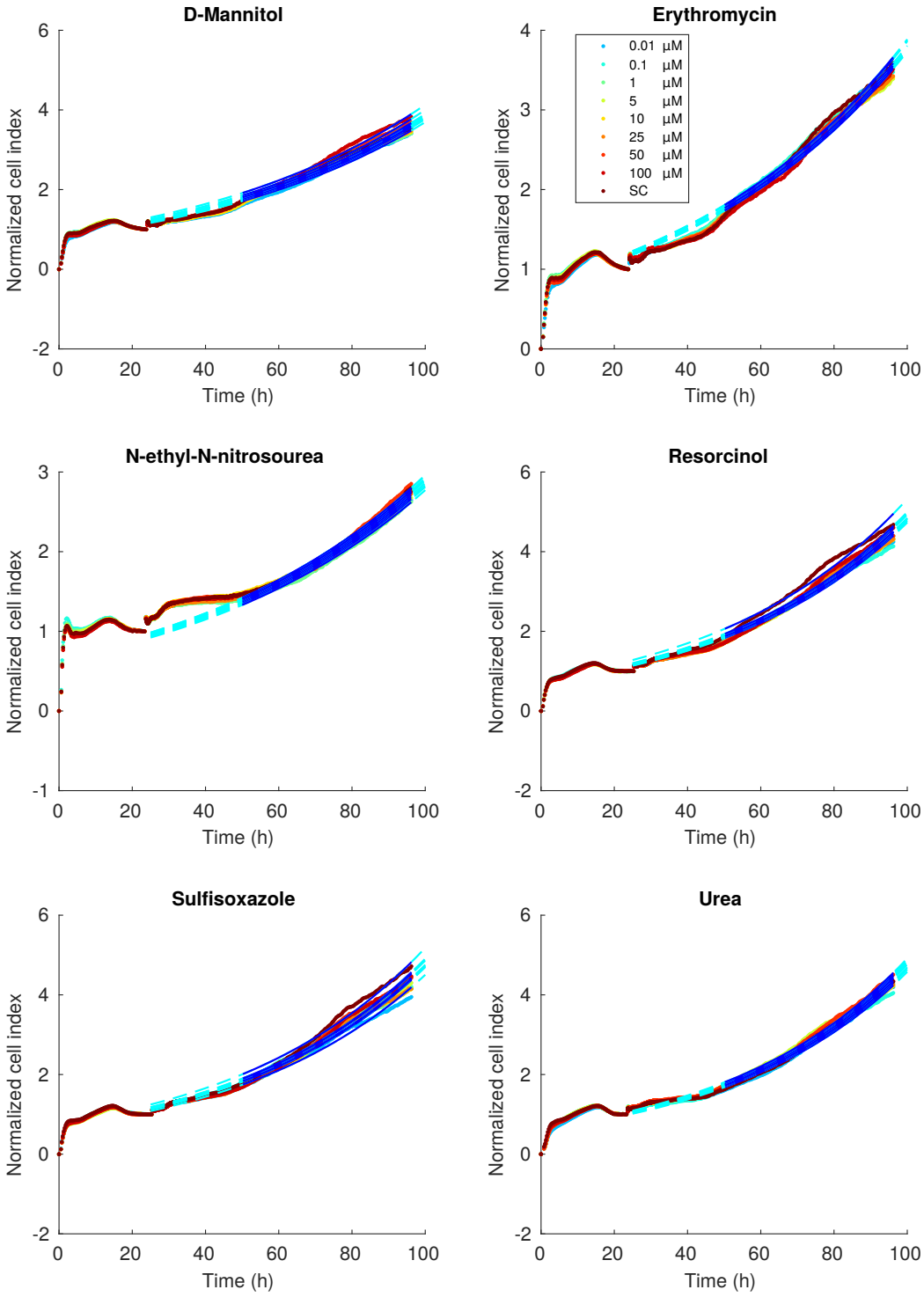

Figure S2: **Time-profiles of the simulated and the experimental data for compounds predicted to be non-toxic.** Figure illustrates the fit of the simulated (in dark blue) and the experimental data (labeled colored markers in the sub-figures). Simulations were performed for the time-period relevant to the cytotoxic phase, which in our study was from 50 h until the end of the experiment. The cyan line indicates the extrapolation of the simulated curves beyond the time-interval of simulations.